Influence of the isospin and hypercharge chemical potentials on the location of the critical end point in the μ_B-T phase diagram of the $SU(3)_L \times SU(3)_R$ chiral quark model

P. Kovács*

Research Group for Statistical and Biological Physics of the Hungarian Academy of Sciences, H-1117 Budapest, Hungary

Zs. Szép†

Research Institute for Solid State Physics and Optics of the Hungarian Academy of Sciences, H-1525 Budapest, Hungary

(Received 8 October 2007; published 14 March 2008)

We investigate the influence of the asymmetric quark matter ($\rho_u \neq \rho_d \neq \rho_s$) on the mass of the quasiparticles and the phase diagram of the chiral quark model parametrized at the one-loop level of the renormalized theory, using the optimized perturbation theory for the resummation of the perturbative series. The effect of various chemical potentials introduced in the grand canonical ensemble is investigated with the method of relativistic many-body theory. The temperature dependence of the topological susceptibility is estimated with the help of the Witten-Veneziano mass formula.

DOI: 10.1103/PhysRevD.77.065016 PACS numbers: 11.10.Wx, 11.30.Rd, 12.39.Fe

I. INTRODUCTION

The study of a system of particles at finite density and temperature is phenomenologically interesting because in heavy ion collision experiments the initial state is such that the chemical potentials μ_B, μ_I, and μ_Y (conjugate to the baryon charge, third component of the isospin, and hypercharge, respectively) are nonvanishing, although the last two are much smaller than the first one. Assuming thermal equilibrium, thermal models show that the strangeness chemical potential in central Si + Au collisions at the Brookhaven AGS experiment was 20%–25% of the baryonic chemical potential for which the best fit gives $\mu_B =$ 540 MeV [1]. For central Pb + Pb collisions at CERN SPS experiments, the value of the strangeness chemical potential was ~25%–30% and that of the isospin chemical potential ~2%–5% of the value of μ_B estimated to be around 233–266 MeV [2,3]. The compressed baryonic matter experiment at FAIR in Darmstadt will explore regions of the QCD phase diagram with moderate temperature up to values of the baryonic density which are comparable with those in the core of neutron stars [4].

In many-body theory chemical potential is introduced to any conserved charge. In heavy ion collision experiments the baryon number, isospin, and hypercharge can be considered conserved due to the short time elapsed between the formation of the fireball and its freeze-out, during which only the strong interactions play an important role, the electroweak interactions being negligible. It is expected that in the very early stage of the fireball's evolution strangeness is abundantly produced in the deconfined phase through gluon-gluon fusion [5], while in the hadronic phase in the vicinity of the transition multimesonic reactions will play an important role in the fast redistribution of strange quarks [6].

The influence of the isospin chemical potential on the chiral phase transition is currently actively investigated because this effect can in principle be tested experimentally. As noticed in [7], using different isotopes of an element in heavy ion collision experiments will vary μ_I keeping μ_B constant. Moreover, the system with real μ_I represents no extra difficulty in lattice field theory compared to the introduction of μ_B. For two flavors the simulations at $\mu_B = 0$ and $\mu_I \neq 0$ are not even affected by the sign problem [8]. For $\mu_I \neq 0$ a generic result coming from effective models of the strongly interacting matter without the $U(1)_A$ anomaly appeared to be the splitting in the μ_B-T plane of the first order transition line into two transition lines. This effect was observed in a random matrix model [9], Nambu-Jona-Lasinio model [10], and strong coupling limit of the staggered lattice QCD [11], all with two flavors and in the three-flavor ladder QCD [12]. This would imply the existence of not only the two phases having $\langle \bar{u}u \rangle \neq 0$, $\langle \bar{d}d \rangle \neq 0$, and $\langle \bar{u}u \rangle = \langle \bar{d}d \rangle = 0$, respectively, but also of a phase with $\langle \bar{u}u \rangle = 0$ and $\langle \bar{d}d \rangle \neq 0$. It was shown in [13,14] that the structure with two transition lines and critical end points ceases to exist for a sufficiently strong $U(1)_A$ breaking, above which the two strongly coupled condensates vanish simultaneously. In a hadron resonance gas model it was found that at fixed baryon chemical potential the pseudocritical temperature of the transition between the hadronic phase and the quark-gluon plasma phase is lowered as either the isospin or the strangeness chemical potential is increased [15].

Because of their phenomenological implications, it is natural to study to what extent these results are present in another low energy effective model, the chiral quark model, widely used for studying the chiral behavior of strongly interacting matter. In the past few years we have

*kpeti@cleopatra.elte.hu
†szepzs@achilles.elte.hu

investigated the thermodynamics of this model for two and three quark flavors at $\mu_B = 0$ and $\mu_B \neq 0$, while leaving $\mu_I = \mu_Y = 0$ [16–19]. As a continuation of these previous studies, in this paper we consider the influence of the chemical potentials on the chiral phase transition up to high values of the isospin chemical potential above which the condensation of pseudoscalar mesons occurs. The pion and kaon condensation phase, which is beyond the scope of our present investigation, was studied both with lattice methods and using effective theories [20–26].

The paper is organized as follows. In Sec. II we present the model, its one-loop parametrization, and the introduction of the chemical potentials. The variation of the location of the critical end point in the presence of μ_I and μ_Y is studied in Sec. III. There we investigate also the temperature and density dependence of the one-loop pole masses of the pseudoscalar mesons. We conclude in Sec. IV.

II. THE $SU(3)_L \times SU(3)_R$ SYMMETRIC CHIRAL QUARK MODEL

The Lagrangian of the model containing explicit symmetry breaking terms is

$$\begin{aligned} L = {} & \tfrac{1}{2}\mathrm{Tr}(\partial_\mu M^\dagger \partial^\mu M + m_0^2 M^\dagger M) - f_1(\mathrm{Tr}(M^\dagger M))^2 \\ & - f_2 \mathrm{Tr}(M^\dagger M)^2 - g(\det(M) + \det(M^\dagger)) + \epsilon_0 \sigma_0 \\ & + \epsilon_3 \sigma_3 + \epsilon_8 \sigma_8 + \bar{\psi}(i\partial\!\!\!/ - g_F M_5)\psi. \end{aligned} \tag{1}$$

The constituent quarks are contained in the field ψ: $\bar{\psi} = (\bar{u}, \bar{d}, \bar{s})$. The two 3×3 complex matrices are defined in terms of the scalar σ_i and pseudoscalar π_i fields as $M = \frac{1}{\sqrt{2}} \sum_{i=0}^{8} (\sigma_i + i\pi_i)\lambda_i$ and $M_5 = \frac{1}{2} \sum_{i=0}^{8} (\sigma_i + i\gamma_5 \pi_i)\lambda_i$, with λ_i: $i = 1 \ldots 8$ the Gell-Mann matrices and $\lambda_0 := \sqrt{\frac{2}{3}}\mathbf{1}$. The fields with well defined quantum numbers are obtained with a block-diagonal transformation $f_\alpha = T_{\alpha i} f_i$, $f \in \{\sigma, \pi\}$, where $T = \mathrm{diag}(1, \tau, 1, \tau, \tau, 1)$ and

$$\tau = \frac{1}{\sqrt{2}} \begin{pmatrix} 1 & -i \\ 1 & i \end{pmatrix}.$$

As α goes from 0 to 8, the components of the scalar and pseudoscalar fields go through σ_0, a_0^+, a_0^-, σ_3, κ^+, κ^-, κ^0, $\bar{\kappa}^0$, σ_8 and π_0, π^+, π^-, π_3, K^+, K^-, K^0, $\bar{K}^0$, π_8, respectively. The physical fields π^0 (neutral pion), η, and η' mesons in the pseudoscalar sector and a_0^0 (neutral a_0), σ, and f_0 in the scalar sector are obtained as linear combinations of the corresponding fields in the two mixing 0, 3, 8 sectors.

In this paper we investigate the pattern of symmetry breaking realized in nature, with the $SU(3)_A \times U(1)_A \times SU(3)_V$ symmetry completely broken; that is, the isospin $SU(2)_V$ is also broken. In addition to the spontaneous symmetry breaking, explicit breaking is also considered with the introduction of external fields for all the diagonal generators of the scalar sector. This results in having three nonvanishing condensates in the broken symmetry phase: $\upsilon_\delta = \langle \sigma_\delta \rangle$, for $\delta = 0, 3, 8$. The condensates determine the tree-level scalar and pseudoscalar masses:

$$\begin{aligned} m^2_{S,\alpha\beta} &= m_0^2 \delta_{\alpha\beta} - 6\tilde{G}_{\alpha\beta\gamma}\upsilon_\gamma + 4\tilde{F}_{\alpha\beta\gamma\delta}\upsilon_\gamma\upsilon_\delta, \\ m^2_{P,\alpha\beta} &= m_0^2 \delta_{\alpha\beta} + 6\tilde{G}_{\alpha\beta\gamma}\upsilon_\gamma + 4\tilde{H}_{\alpha\beta,\gamma\delta}\upsilon_\gamma\upsilon_\delta. \end{aligned} \tag{2}$$

The tensors appearing above arise after the evaluation of the trace in (1) and the transformation of the fields to the basis with good quantum numbers. The connection between these coupling tensors and the original ones appearing in (1) which can be found in [27,28] is given by

$$\begin{aligned} \tilde{G}_{\alpha\beta\gamma} &= \sum_{i,j,k=0}^{8} G_{ijk} T^{-1}_{i\alpha} T^{-1}_{j\beta} T^{-1}_{k\gamma}, \\ \tilde{H}_{\alpha\beta,\gamma\delta} &= \sum_{i,j,k,l=0}^{8} H_{ij,kl} T^{-1}_{i\alpha} T^{-1}_{j\beta} T^{-1}_{k\gamma} T^{-1}_{l\gamma}, \\ \tilde{F}_{\alpha\beta\gamma\delta} &= \sum_{i,j,k,l=0}^{8} F_{ijkl} T^{-1}_{i\alpha} T^{-1}_{j\beta} T^{-1}_{k\gamma} T^{-1}_{l\gamma}. \end{aligned} \tag{3}$$

The transformations preserve the symmetry structure of the tensors; that is, $\tilde{G}_{\alpha\beta\gamma}$ and $\tilde{F}_{\alpha\beta\gamma\delta}$ are completely symmetric, and $\tilde{H}_{\alpha\beta,\gamma\delta}$ is symmetric upon the interchange of two indices which are on the same side of the comma.

The tree-level mass square matrices are not diagonal in the 0, 3, 8 subspace, but since they are real and symmetric, diagonalization is achieved with an orthogonal transformation. The tree-level orthogonal matrices in the scalar and pseudoscalar sectors are denoted with O_S and O_P, respectively. Denoting the eigenvalues of the pseudoscalar and the scalar 3×3 mass matrices in the 0, 3, 8 sector with $\lambda_{P,\{\min,\mathrm{mid},\max\}}$ and $\lambda_{S,\{\min,\mathrm{mid},\max\}}$, the tree-level masses of the mesons are as follows:

$$\begin{aligned} m^2_{\pi^+} &= m^2_{\pi^-} = m^2_{P,12}, & m^2_{a_0^+} &= m^2_{a_0^-} = m^2_{S,12}, \\ m^2_{\pi^0} &= \lambda_{P,\min}, & m^2_{a_0^0} &= \lambda_{S,\mathrm{mid}}, \\ m^2_{K^+} &= m^2_{K^-} = m^2_{P,45}, & m^2_{\kappa^+} &= m^2_{\kappa^-} = m^2_{S,45}, \\ m^2_{K^0} &= m^2_{\bar{K}^0} = m^2_{P,67}, & m^2_{\kappa^0} &= m^2_{\bar{\kappa}^0} = m^2_{S,67}, \\ m^2_{\eta} &= \lambda_{P,\mathrm{mid}}, & m^2_{\sigma} &= \lambda_{S,\min}, \\ m^2_{\eta'} &= \lambda_{P,\max}, & m^2_{f_0} &= \lambda_{S,\max}. \end{aligned} \tag{4}$$

Note that some of the tree-level masses of scalars and pseudoscalars coincide. As we will see, the introduction of isospin and hypercharge chemical potentials distinguishes between the particles, and as a result all the one-loop pole masses will be different for $\mu_I, \mu_Y \neq 0$.

The tree-level fermion masses are

$$M_u = \frac{g_F}{\sqrt{12}}(\sqrt{2}v_0 + \sqrt{3}v_3 + v_8),$$
$$M_d = \frac{g_F}{\sqrt{12}}(\sqrt{2}v_0 - \sqrt{3}v_3 + v_8), \quad (5)$$
$$M_s = \frac{g_F}{\sqrt{12}}(\sqrt{2}v_0 - 2v_8).$$

The evolution of the condensates with the temperature or/and the chemical potentials is determined by the three equations of state

$$0 = \left\langle \frac{\partial L}{\partial \sigma_0} \right\rangle$$
$$= m^2 v_0 - \frac{c}{2\sqrt{6}}(2v_0^2 - v_3^2 - v_8^2) + \frac{1}{3}(3f_1 + f_2)v_0^3 + (f_1 + f_2)(v_3^2 + v_8^2)v_0 + \frac{f_2}{3\sqrt{2}}(3v_3^2 - v_8^2)v_8 - \varepsilon_0$$
$$- \sum_{\substack{f\in\{\sigma,\pi\}\\ \alpha=1,2,4...7}} t^0_{f,\alpha}\langle f^\dagger_\alpha f_\alpha\rangle - 3\sum_{\gamma\in\{0,3,8\}}[(O_S^T S_0 O_S)_{\gamma\gamma}\langle\sigma_\gamma\sigma_\gamma\rangle + (O_P^T P_0 O_P)_{\gamma\gamma}\langle\pi_\gamma\pi_\gamma\rangle] + \frac{g_F}{\sqrt{6}}N_c(\langle\bar{u}u\rangle + \langle\bar{d}d\rangle + \langle\bar{s}s\rangle), \quad (6)$$

$$0 = \left\langle \frac{\partial L}{\partial \sigma_3} \right\rangle$$
$$= \left(m^2 - \frac{c}{\sqrt{3}}v_8 + \frac{c}{\sqrt{6}}v_0 + \left(f_1 + \frac{f_2}{2}\right)(v_3^2 + v_8^2) + (f_1 + f_2)v_0^2 + \sqrt{2}f_2 v_0 v_8\right)v_3 - \epsilon_3 - \sum_{\substack{f\in\{\sigma,\pi\}\\ \alpha=1,2,4...7}} t^3_{f,\alpha}\langle f^\dagger_\alpha f_\alpha\rangle$$
$$- 3\sum_{\gamma\in\{0,3,8\}}[(O_S^T S_3 O_S)_{\gamma\gamma}\langle\sigma_\gamma\sigma_\gamma\rangle + (O_P^T P_3 O_P)_{\gamma\gamma}\langle\pi_\gamma\pi_\gamma\rangle] + \frac{g_F}{2}N_c(\langle\bar{u}u\rangle - \langle\bar{d}d\rangle), \quad (7)$$

$$0 = \left\langle \frac{\partial L}{\partial \sigma_8} \right\rangle$$
$$= m^2 v_8 + \frac{c}{\sqrt{6}}v_0 v_8 + \frac{c}{2\sqrt{3}}(v_8^2 - v_3^2) + \left(f_1 + \frac{f_2}{2}\right)(v_8^2 + v_3^2)v_8 + \frac{f_2}{\sqrt{2}}(v_3^2 - v_8^2)v_0 + (f_1 + f_2)v_0^2 v_8 - \varepsilon_8$$
$$- \sum_{\substack{f\in\{\sigma,\pi\}\\ \alpha=1,2,4...7}} t^8_{f,\alpha}\langle f^\dagger_\alpha f_\alpha\rangle - 3\sum_{\gamma\in\{0,3,8\}}[(O_S^T S_8 O_S)_{\gamma\gamma}\langle\sigma_\gamma\sigma_\gamma\rangle + (O_P^T P_8 O_P)_{\gamma\gamma}\langle\pi_\gamma\pi_\gamma\rangle] + \frac{g_F}{2\sqrt{3}}N_c(\langle\bar{u}u\rangle + \langle\bar{d}d\rangle - 2\langle\bar{s}s\rangle), \quad (8)$$

where in the mixing sector σ_γ stands for σ, a_0^0, f_0 and similarly π_γ denotes π^0, η, η' as $\gamma = 0, 3, 8$, respectively. $f^\dagger_\alpha$ denotes the antiparticle of f_α; that is, e.g. for $f = \sigma$ and $\alpha = 1$ one has $\sigma_1 = a_0^+$ and $\sigma_1^\dagger = a_0^-$. In this notation $\langle f^+_\alpha f_\alpha\rangle = T_B^\beta(m_{f_\alpha})$, $\langle\bar{q}q\rangle = -4m_q T_F^\beta(m_q)$, where $T_B^\beta(m_{f_\alpha})$ and $T_F^\beta(m_q)$ stand for the bosonic and the fermionic tadpole integrals, respectively. These integrals are given in Appendix B of [19]. The coefficients $t^\gamma_{f,\alpha}$ are listed in Table I. In the mixing sector, that is for $\gamma = 0, 3, 8$, the 3×3 matrices read

$$S_\gamma = \tilde{G}_0 - \tfrac{4}{3}v_0\tilde{F}_{\gamma 0} - \tfrac{4}{3}v_3\tilde{F}_{\gamma 3} - \tfrac{4}{3}v_8\tilde{F}_{\gamma 8},$$
$$P_\gamma = \tilde{G}_0 + \tfrac{4}{3}v_0\tilde{H}_{\gamma 0} + \tfrac{4}{3}v_3\tilde{H}_{\gamma 3} + \tfrac{4}{3}v_8\tilde{H}_{\gamma 8}, \quad (9)$$

with the definition $(\tilde{G}_\gamma)_{\alpha\beta} \equiv \tilde{G}_{\gamma\alpha\beta}$, $(\tilde{F}_{\gamma\delta})_{\alpha\beta} \equiv \tilde{F}_{\alpha\beta\gamma\delta}$, and $(\tilde{H}_{\gamma\delta})_{\alpha\beta} \equiv \tilde{H}_{\alpha\beta,\gamma\delta}$. All the indices run through 0, 3, or 8.

A. One-loop parametrization of the model at zero temperature and density

One has some freedom in choosing the set of equations which determines the 13 parameters of the model, namely, m_0^2, f_1, f_2, g, g_F, v_0, v_3, v_8, ϵ_0, ϵ_3, ϵ_8 and l_f, l_b. These last two parameters are the fermionic and bosonic renormalization scales. For the parametrization we follow the

TABLE I. The $t^\gamma_{f,\alpha}$ coefficients appearing in the equations of state (6)–(8). The summation index δ goes over 0, 3, 8.

α	$t^\gamma_{\sigma,\alpha}$	α	$t^\gamma_{\pi,\alpha}$
a_0^-	$3\tilde{G}_{\gamma 21} - 4\tilde{H}_{\gamma 21\delta v\delta}$	π^-	$3\tilde{G}_{\gamma 21} - 4\tilde{F}_{\gamma 21\delta v\delta}$
a_0^+	$3\tilde{G}_{\gamma 12} - 4\tilde{H}_{\gamma 12\delta v\delta}$	π^+	$3\tilde{G}_{\gamma 12} - 4\tilde{F}_{\gamma 12\delta v\delta}$
κ^-	$3\tilde{G}_{\gamma 54} - 4\tilde{H}_{\gamma 54\delta v\delta}$	K^-	$3\tilde{G}_{\gamma 54} - 4\tilde{F}_{\gamma 54\delta v\delta}$
κ^+	$3\tilde{G}_{\gamma 45} - 4\tilde{H}_{\gamma 45\delta v\delta}$	K^+	$3\tilde{G}_{\gamma 45} - 4\tilde{F}_{\gamma 45\delta v\delta}$
$\bar{\kappa}^0$	$3\tilde{G}_{\gamma 76} - 4\tilde{H}_{\gamma 76\delta v\delta}$	$\bar{K}^0$	$3\tilde{G}_{\gamma 76} - 4\tilde{F}_{\gamma 76\delta v\delta}$
κ^0	$3\tilde{G}_{\gamma 67} - 4\tilde{H}_{\gamma 67\delta v\delta}$	K^0	$3\tilde{G}_{\gamma 67} - 4\tilde{F}_{\gamma 67\delta v\delta}$

method described in [19] where the renormalization of the model was also discussed. The only difference in the present case is the appearance of v_3 and ϵ_3. Since at zero temperature and densities the effect of isospin breaking is small, we use the same values for l_f and l_b as in [19] where these were determined by minimizing the deviation of the predicted mass spectrum from the physical one. The external fields are determined from the equations of state (6)–(8) once the remaining 8 parameters are known.

In order to avoid the appearance of negative propagator mass squares in the one-loop finite temperature calculations in the broken symmetry phase, we use the optimized perturbation theory of Ref. [29]. This amounts to replacing the mass parameter $-m_0^2$ in the Lagrangian with an effective, eventually temperature-dependent, mass parameter m^2:

$$\begin{aligned} L_{\text{mass}} &= \tfrac{1}{2}m^2 \text{Tr}M^\dagger M - \tfrac{1}{2}(m_0^2 + m^2)\text{Tr}M^\dagger M \\ &\equiv \tfrac{1}{2}m^2 \text{Tr}M^\dagger M - \tfrac{1}{2}\Delta m^2 \text{Tr}M^\dagger M. \end{aligned} \tag{10}$$

The counterterm Δm^2 is taken into account first at the one-loop level, while m^2 will replace m_0^2 in all the tree-level masses and is determined using the criterion of fastest apparent convergence (FAC). We have chosen to implement this criterion by requiring that for π^+ the one-loop mass calculated at vanishing external momentum stays equal to the tree-level mass ($M_{\pi^+} = m_{\pi^+}$). We have checked that imposing this equation for the neutral pion rather than the charged one results in no significant changes in the parameters. We note here that we were forced to use the definition $M_{\pi^+}^2 = -iG^{-1}(p = 0)$ instead of defining the one-loop mass as the pole of the propagator because in this latter case the solution to the gap equation, to be presented below, ceases to exist above a certain temperature, in accordance with previous investigations using the optimized perturbation theory [18,29].

As described in detail in [19], with the application of FAC one can eliminate the effective mass parameter m^2 in favor of the tree-level pion mass $m_{\pi^+}^2$ in all the other tree-level masses of the propagators used to calculate the one-loop self-energies:

$$\begin{aligned} m^2 = m_{\pi^+}^2 &+ \frac{c}{\sqrt{6}}v_0 - \frac{c}{\sqrt{3}}v_8 - \frac{\sqrt{2}}{3}f_2 v_0 v_8 - \left(f_1 + \frac{f_2}{3}\right)v_0^2 \\ &- \left(f_1 + \frac{3f_2}{2}\right)v_3^2 - \left(f_1 + \frac{f_2}{6}\right)v_8^2. \end{aligned} \tag{11}$$

In this way one obtains the following gap equation:

$$\begin{aligned} m_{\pi^+}^2 = &-m_0^2 - \frac{c}{\sqrt{6}}v_0 + \frac{c}{\sqrt{3}}v_8 + \frac{\sqrt{2}}{3}f_2 v_0 v_8 \\ &+ \left(f_1 + \frac{f_2}{3}\right)v_0^2 + \left(f_1 + \frac{3f_2}{2}\right)v_3^2 + \left(f_1 + \frac{f_2}{6}\right)v_8^2 \\ &+ \text{Re}\Sigma_{\pi^+}(p^2 = 0, m_i^2(m_{\pi^+}^2)), \end{aligned} \tag{12}$$

where Σ_{π^+} denotes the self-energy of π^+ shown diagrammatically in Fig. 1. Equation (12) is the first from a set of four coupled nonlinear equations which determines m_0^2, f_1, f_2, g, if one knows g_F, v_0, v_3, v_8. Two further equations of the set are given by the one-loop equation for the η and K^+ pole masses:

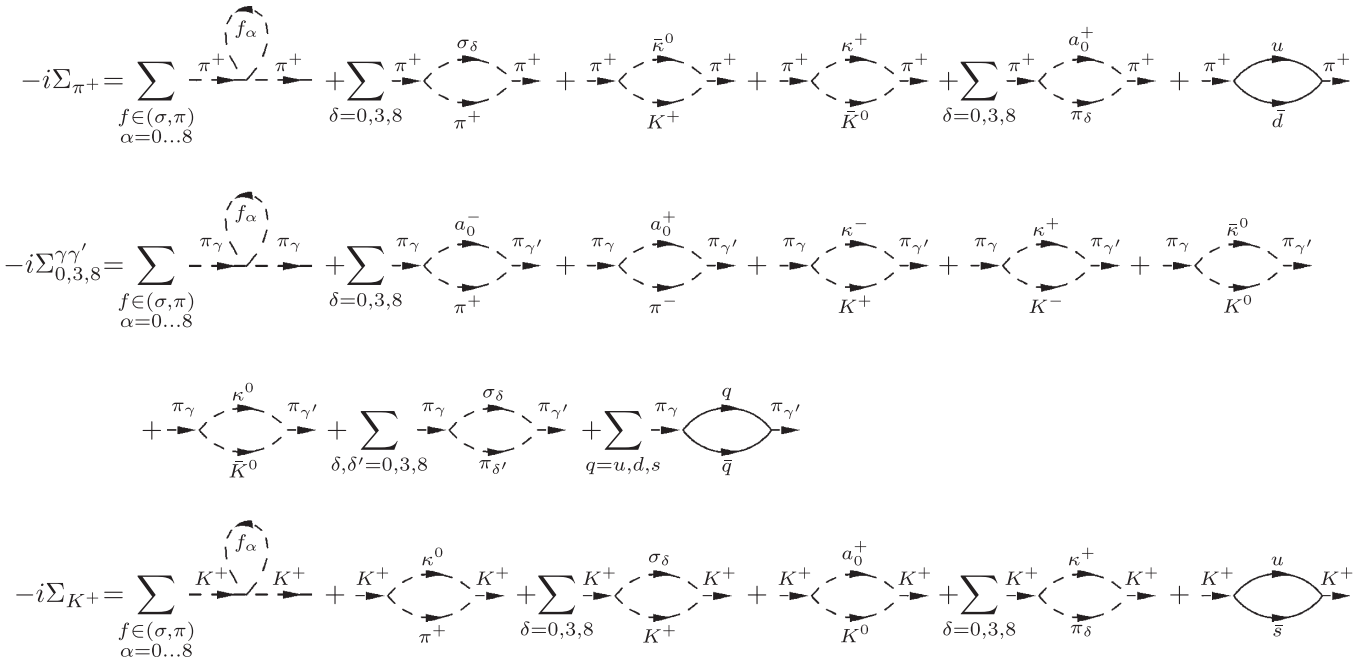

FIG. 1. Diagrammatic representation of the one-loop pseudoscalar self-energies used for the parametrization. The label associated to the line denotes the propagating particle.

$$M_\eta^2 = -m_0^2 + [\tilde{O}_P^T(\mathcal{M}_{\text{tree}}^2 + \text{Re}\Sigma_{0,3,8}(p^2 = M_\eta^2))\tilde{O}_P]_{22}, \tag{13}$$

$$\begin{aligned} M_{K^+}^2 = & -m_0^2 - \frac{c}{\sqrt{6}}v_0 + \frac{c}{2}v_3 - \frac{c}{2\sqrt{3}}v_8 + \frac{f_2}{\sqrt{6}}v_0v_3 \\ & - \frac{f_2}{3\sqrt{2}}v_0v_8 + \frac{2f_2}{\sqrt{3}}v_3v_8 + \left(f_1 + \frac{f_2}{3}\right)v_0^2 \\ & + \left(f_1 + \frac{f_2}{2}\right)v_3^2 + \left(f_1 + \frac{7f_2}{6}\right)v_8^2 \\ & + \text{Re}\Sigma_{K^+}(p^2 = M_{K^+}^2), \end{aligned} \tag{14}$$

where $\mathcal{M}_{\text{tree}}^2$ is the tree-level mass squared matrix of the mixing sector without the mass parameter m^2, the orthogonal matrix $\tilde{O}_P$ diagonalizes the expression in the round bracket, and $\Sigma_{0,3,8}$ is the self-energy matrix of the pseudoscalar mixing sector. This matrix is determined numerically. The last equation in the set is the FAC criterion for the kaon, which requires $\text{Re}\Sigma_{K^+}(p^2 = M_{K^+}^2) - \Delta m^2 = 0$.

The parameters g_F, v_0, v_3, v_8 are determined as follows. A linear combination of v_0 and v_8 is determined by the tree-level partially conserved axial-vector current relation for the pion decay constant (see the Appendix of [28])

$$f_\pi := d_{11a}v_a = \sqrt{\frac{2}{3}}v_0 + \frac{1}{\sqrt{3}}v_8. \tag{15}$$

One can see from (5) that the same linear combination enters the expression of the average mass of the two light constituent quarks, so that the Yukawa coupling is given by $g_F = (M_u + M_d)/f_\pi$. Another linear combination of v_0 and v_8 appears in the expression of M_s in (5) which together with the partially conserved axial-vector current relation (15) determines v_0 and v_8:

$$\begin{aligned} v_0 &= \sqrt{\frac{2}{3}}f_\pi\left(1 + \frac{M_s}{M_u + M_d}\right), \\ v_8 &= \frac{1}{\sqrt{3}}f_\pi\left(1 - \frac{2M_s}{M_u + M_d}\right). \end{aligned} \tag{16}$$

The remaining parameter, v_3, is obtained by requiring that the difference between the tree-level masses of π^+ and π^0 equals the physical value (Δm_π):

$$-[O_P^T\mathcal{M}_{\text{tree}}^2O_P]_{11} = (\Delta m_\pi)^2. \tag{17}$$

This equation has two roots for v_3, a negative and a positive one. The positive root would give $m_{K^0} < m_{K^+}$ for the kaon masses. Since the opposite relation holds in nature, we choose the negative solution which is the physically valid one.

We use the following values for the physical quantities: $m_{\pi^+} = 139.57$ MeV, $\Delta m_\pi = 4.594$ MeV, $M_{K^+} = 493.677$ MeV, $M_\eta = 547.8$ MeV, $f_\pi = 93$ MeV, $(M_u + M_d)/2 = 313$ MeV, $M_s = 530$ MeV, and in addition $l_b = 520$ MeV and $l_f = 1210$ MeV for the two renormalization scales.

B. Introduction of the chemical potentials

The introduction of the chemical potential for a system with a set of conserved charge operators is reviewed below. For vanishing external fields the Lagrangian (1) is invariant under the following global vector transformations:

$$\begin{aligned} M &\to e^{-i\alpha_G G}Me^{i\alpha_G G} = M - i\alpha_G[G, M] + \mathcal{O}(\alpha_G^2), \\ \psi &\to e^{-i\alpha_G G}\psi = \psi - i\alpha_G\psi + \mathcal{O}(\alpha_G^2), \end{aligned} \tag{18}$$

where G denotes the representation of the baryon (B), third component of the isospin (I), and hypercharge (Y) operators which are related to the diagonal generators as $B = \frac{1}{\sqrt{6}}\lambda_0$, $I = \frac{1}{2}\lambda_3$, and $Y = \frac{1}{\sqrt{3}}\lambda_8$. The coefficients in front of the diagonal matrices are chosen to obtain the right quantum numbers when applying the operators on the quark fields. The consequence of this symmetry is the existence of conserved Noether vector-currents

$$\begin{aligned} J_\mu^G = & -\frac{\delta L}{\delta(\partial^\mu M)_{ij}}i[G, M]_{ji} - \frac{\delta L}{\delta(\partial^\mu M^\dagger)_{ij}}i[G, M^\dagger]_{ji} \\ & - \frac{\delta L}{\delta(\partial^\mu\psi_i)}iG_{ij}\psi_j. \end{aligned} \tag{19}$$

The conserved charge is defined as $Q^G = \int d^3x J_0^G(x)$. In terms of particle number operators the conserved baryon, isospin, and hypercharges read as

$$Q^B = \tfrac{1}{3}(N_u + N_d + N_s - N_{\bar{u}} - N_{\bar{d}} - N_{\bar{s}}), \tag{20}$$

$$\begin{aligned} Q^I = & \tfrac{1}{2}(N_u - N_{\bar{u}} - N_d + N_{\bar{d}} + N_{\kappa^+} - N_{\kappa^-} + N_{\bar{\kappa}^0} - N_{\kappa^0} \\ & + N_{K^+} - N_{K^-} + N_{\bar{K}^0} - N_{K^0}) + N_{a_0^+} - N_{a_0^-} \\ & + N_{\pi^+} - N_{\pi^-}, \end{aligned} \tag{21}$$

$$\begin{aligned} Q^Y = & \tfrac{1}{3}(N_u - N_{\bar{u}} + N_d - N_{\bar{d}} - 2N_s + 2N_{\bar{s}}) + N_{\kappa^+} \\ & - N_{\kappa^-} + N_{\kappa^0} - N_{\bar{\kappa}^0} + N_{K^+} - N_{K^-} + N_{K^0} - N_{\bar{K}^0}. \end{aligned} \tag{22}$$

Note the different sign of N_{K^0}, $N_{\bar{K}^0}$, N_{κ^0}, $N_{\bar{\kappa}^0}$ in Q^I relative to Q^Y. This is because the particles K^0, $\bar{K}^0$, κ^0, $\bar{\kappa}^0$ fall into different doublets from the point of view of the I_3 and Y quantum numbers: K^0, K^+ and K^-, $\bar{K}^0$ form an I_3 doublet while K^0, K^- and K^+, $\bar{K}^0$ form a Y doublet (likewise for scalars).

The statistical density matrix of the system is given by

$$\rho = \exp[-\beta(H - \mu_G Q^G)], \tag{23}$$

with G going over B, I, Y in the summation over this index. Using (20)–(22) one can rewrite (23) by regrouping the terms in the exponent according to different number operators and obtain $\rho = \exp[-\beta(H - \mu_i N_i)]$, where i goes over all the particles with I_3, $Y \neq 0$ to which the following

chemical potentials were introduced in terms of μ_B, μ_I, μ_Y:

$$\begin{aligned}
\mu_u &= -\mu_{\bar{u}} = \tfrac{1}{3}\mu_B + \tfrac{1}{2}\mu_I + \tfrac{1}{3}\mu_Y, \\
\mu_d &= -\mu_{\bar{d}} = \tfrac{1}{3}\mu_B - \tfrac{1}{2}\mu_I + \tfrac{1}{3}\mu_Y, \\
\mu_s &= -\mu_{\bar{s}} = \tfrac{1}{3}\mu_B - \tfrac{2}{3}\mu_Y, \\
\mu_{a_0^+} &= \mu_{\pi^+} = -\mu_{a_0^-} = -\mu_{\pi^-} = \mu_I, \\
\mu_{\kappa^+} &= \mu_{K^+} = -\mu_{\kappa^-} = -\mu_{K^-} = \tfrac{1}{2}\mu_I + \mu_Y, \\
\mu_{\kappa^0} &= \mu_{K^0} = -\mu_{\bar{\kappa}^0} = -\mu_{\bar{K}^0} = -\tfrac{1}{2}\mu_I + \mu_Y.
\end{aligned} \tag{24}$$

The particles with $I_3 = Y = 0$ (π^0, η, η', a_0^0, σ, and f_0) do not contribute to the conserved charges, and in consequence no chemical potential is introduced for them. By looking at (24) one can see that different members of a given multiplet (e.g. π^+ and π^-) acquire a different combination of the baryon, isospin, and hypercharge chemical potentials, which means that the chemical potentials remove completely the degeneracy between the members of the multiplets which we observe in the vacuum, both at the tree and one-loop level. We have to keep track of the effect of 21 individually different particles, which makes things more complicated than in previous studies of this model.

The effect of the chemical potentials is taken into account through the propagators which are introduced using the definition familiar from the theory of many-body systems. The relativistic formalism was developed in [30] and is reviewed in the Appendix, where the calculation of the self-energy using the finite-density Green's function is also sketched.

In order to see explicitly that the particle and its antiparticle reflect differently the presence of a finite-density medium, we give here the tree-level propagators of K^+ and K^-:

$$\begin{aligned}
G_{K^+}(k) = \frac{i}{2E_{\mathbf{k}}}\Bigg[&\frac{1+n_{K^+}(E_{\mathbf{k}})}{k_0 - E_{\mathbf{k}} + i\epsilon} - \frac{n_{K^+}(E_{\mathbf{k}})}{k_0 - E_{\mathbf{k}} - i\epsilon} \\
&- \frac{1+n_{K^-}(E_{\mathbf{k}})}{k_0 + E_{\mathbf{k}} - i\epsilon} + \frac{n_{K^-}(E_{\mathbf{k}})}{k_0 + E_{\mathbf{k}} + i\epsilon}\Bigg], \\
G_{K^-}(k) = \frac{i}{2E_{\mathbf{k}}}\Bigg[&\frac{1+n_{K^-}(E_{\mathbf{k}})}{k_0 - E_{\mathbf{k}} + i\epsilon} - \frac{n_{K^-}(E_{\mathbf{k}})}{k_0 - E_{\mathbf{k}} - i\epsilon} \\
&- \frac{1+n_{K^+}(E_{\mathbf{k}})}{k_0 + E_{\mathbf{k}} - i\epsilon} + \frac{n_{K^+}(E_{\mathbf{k}})}{k_0 + E_{\mathbf{k}} + i\epsilon}\Bigg],
\end{aligned} \tag{25}$$

where $n_{K^\pm}(E_{\mathbf{k}}) = \frac{1}{e^{\beta(E_{\mathbf{k}} - \mu_{K^\pm})} - 1}$ and $E_{\mathbf{k}} = \sqrt{\mathbf{k}^2 + m_{K^\pm}^2}$. The interpretation of the terms on the right-hand side of (25) is as follows (from left to right): addition of a particle, removal of a particle, addition of an antiparticle, removal of an antiparticle. Note that in the propagator of the K^+ the particle is K^+ and the antiparticle is K^-, while in the propagator of the K^- the particle is K^- and the antiparticle is K^+.

For all the other scalar and pseudoscalar fields the propagators can be written analogously using the chemical potentials defined in (24). For the fermions the propagators are given in the Appendix.

III. THERMODYNAMICS OF THE MODEL AT FINITE DENSITY

A. The influence of μ_I and μ_Y on the CEP

With the parameters fixed in the previous section, we can solve the model at finite temperature and density using the formalism described in Sec. II B and in the Appendix. One calculates the 1-loop integrals entering the finite temperature and density version of the equations which determine the state of the system: the three equations of state (6)–(8) and the gap equation for m_{π^+} (12). The relevant integrals are given in the Appendix. An observed smooth variation of the order parameters with the intensive parameter (T, or $\mu_{B,I,Y}$) indicates an analytic crossover type transition. A first order phase transition is signaled by the multivaluedness of either one of the three condensates in a given range of variation of the intensive parameter. The point where by varying some parameter(s) the nature of the phase transition changes from crossover to first order one corresponds to a second order phase transition.

The critical end point (CEP) is a second order phase-transition point on the μ_B-T plane where by increasing μ_B the phase transition as a function of T changes from crossover to first order (μ_I and μ_Y are kept constant). At vanishing μ_I and μ_Y the CEP is located in the point $(T, \mu_B)_{\mathrm{CEP}} = (63.08, 960.8)$ MeV. The pseudocritical temperature at vanishing chemical potentials is $T_c(\mu_{B,I,Y} = 0) = 157.98$ MeV.

Here it is important to note that, with the explicit isospin breaking taken into account, these values have significantly changed with respect to those obtained without isospin breaking at all (neither explicit nor spontaneous): $(T, \mu_B)_{\mathrm{CEP}} = (74.83, 895.38)$ MeV and $T_c(\mu_{B,I,Y} = 0) = 154.84$ MeV [19]. At first sight this is surprising since we have seen that at $T = \mu = 0$ the effect of the explicit symmetry breaking is minimal. The difference is due to the behavior of the v_3 with the temperature. Without explicit isospin symmetry breaking v_3 is identically zero for $\mu_I = 0$. When $\epsilon_3 \neq 0$, one can see by looking at the reference curve of Fig. 2 that with increasing temperature v_3 is decreasing significantly compared to its $T = 0$ value and reaches a minimum around the phase-transition point where the influence of v_3 becomes the strongest. The left-hand panel of Fig. 2 shows that the baryochemical potential magnifies this effect, implying that approaching the CEP the influence of v_3 is even stronger. According to our conjecture made in [19] that a smoother crossover at $\mu_B = 0$ will require a larger value of μ_B to turn the phase transition in T into a first order one, implying a larger value of $\mu_{B,\mathrm{CEP}}$, we can expect that the larger value of $\mu_{B,\mathrm{CEP}}$ in the case of the explicit isospin breaking com-

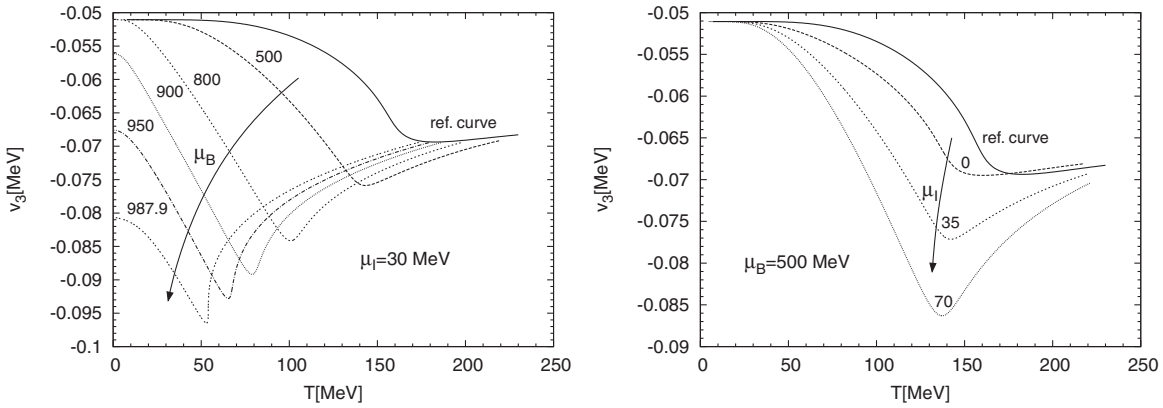

FIG. 2. The generic temperature dependence of v_3 for a crossover transition: on the left-hand side μ_B changes and $\mu_I = 30$ MeV; on the right-hand side μ_I changes while $\mu_B = 500$ MeV. On both panels the reference curve (ref. curve) refers to the case $\mu_B = \mu_I = \mu_Y = 0$.

pared to the case in which the isospin breaking is absent corresponds to a higher value of the width of the chiral susceptibility $\Delta T_c(x\chi)$. Indeed, by looking at Fig. 3 one can see that in the case with explicit isospin symmetry breaking $\Delta T_c(x\chi)$ increased by $\sim$20%, approaching the value of $\Delta T_c(\chi_{\bar{\psi}\psi}) = 28(5)(1)$ MeV at $\mu_I = 0$. This value was obtained on the lattice in Ref. [31] after the extrapolation in the continuum limit was done, though in this lattice investigation the effect of isospin breaking was not taken into account. It would be interesting to see whether a similar effect is produced on lattice when $m_u \neq m_d$.

Varying μ_I and μ_Y the location of the CEP in the μ_B-T plane changes. Figure 4 shows the surfaces swept by the two coordinates of the CEP as functions of μ_I and μ_Y. One can see that μ_Y has practically no influence on $T_{\rm CEP}$, which decreases very slowly, while with its increase $\mu_{B,\rm CEP}$ significantly decreases. The increase of μ_I pushes the CEP toward higher values of $\mu_{B,\rm CEP}$ and lower values of $T_{\rm CEP}$. This behavior is in accordance with what was previously written on the influence of v_3 on the CEP at $\mu_I = 0$, since by looking at the left-hand side of Fig. 2 one sees that at finite μ_I the isospin condensate v_3 increases even more with the temperature.

One can gain intuition on the way the chemical potentials μ_I and μ_Y influence the coordinates of the CEP by attempting a simple interpretation of our results in terms of generalized Clausius-Clapeyron equations applied to our system. The particle number and entropy densities of the two coexisting phases will be determined assuming an ideal gas of the quasiparticle degrees of freedom, which differ only in their respective masses on the two sides of the phase coexisting curves. The Clausius-Clapeyron equations successfully describe the slopes of phase coexistence curves of strong matter as functions of various chemical potentials and quark masses [11,32,33]. They are derived from the Gibbs-Duhem relation which connects the variation of the intensive thermodynamical parameters of a macroscopic system:

$$dp = sdT + n_B d\mu_B + n_I d\mu_I + n_Y d\mu_Y. \tag{26}$$

Here n_B, n_Y, n_I are the particle number densities, and s is the entropy density. Keeping the pressure plus any other two intensive parameters constant one finds the following set of conditions for the phase coexistence when one varies the remaining two intensive parameters along the coexistence "surface":

$$\begin{aligned} \left.\frac{dT}{d\mu_B}\right|_{\mu_Y,\mu_I} &= -\frac{\Delta n_B}{\Delta s}, \qquad \left.\frac{dT}{d\mu_Y}\right|_{\mu_B,\mu_I} = -\frac{\Delta n_Y}{\Delta s}, \\ \left.\frac{dT}{d\mu_I}\right|_{\mu_B,\mu_Y} &= -\frac{\Delta n_I}{\Delta s}, \qquad \left.\frac{d\mu_B}{d\mu_Y}\right|_{T,\mu_I} = -\frac{\Delta n_Y}{\Delta n_B}, \\ \left.\frac{d\mu_B}{d\mu_I}\right|_{T,\mu_Y} &= -\frac{\Delta n_I}{\Delta n_B}. \end{aligned} \tag{27}$$

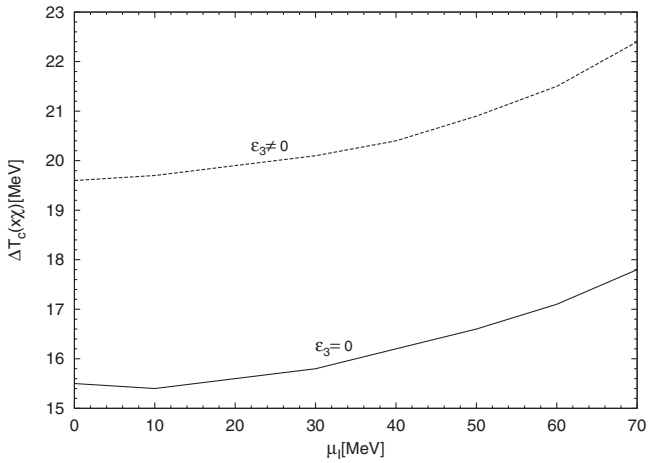

FIG. 3. The width of the peak of the chiral susceptibility $\Delta T_c(x\chi)$ as a function of the isospin chemical potential with (without) explicit symmetry breaking external field $\epsilon_3 \neq 0$ ($\epsilon_3 = 0$). In the chiral quark model $\chi = dx/d\epsilon_x$ where $x = \sqrt{2/3}(v_0 - v_8)$ is the nonstrange condensate, $\epsilon_x = \sqrt{2/3}(\epsilon_0 - \epsilon_8)$, and as shown in [19] $\chi_{\bar{\psi}\psi} \sim x\chi$.

In the above equations Δ refers to the difference of the values of a given extensive quantity in the symmetric and broken symmetry phase. In the two coexisting phases the relevant particle number and/or entropy densities ($n_G, G = B, I, Y$, and s) can be calculated from the partition function using the formulas $n_G = TV^{-1}\partial \ln Z/\partial \mu_G$ and $s = V^{-1}\partial(T \ln Z)/\partial T$. Our simplified picture of the composition of the two phases in terms of noninteracting mixtures of 15 quasiparticles is given by

$$\ln Z = V\sum_i \gamma_i(2s_i + 1) \times \int \frac{d^3\mathbf{p}}{(2\pi)^3}[\beta\omega_i + \ln(1 + \alpha_i e^{-\beta(\omega_i - \mu_i)}) + \ln(1 + \alpha_i e^{-\beta(\omega_i + \mu_i)})], \quad (28)$$

where $i \in \pi^\pm, \pi^0, K^\pm, K^0, \eta, \eta', a_0^\pm, a_0^0, \kappa^\pm, \kappa^0, \sigma, f_0, u, d, s$ and for fermions one has $\gamma_i = N_c$, $\alpha_i = 1$, and $s_i = 1/2$, while for bosons one has $\gamma_i = \alpha_i = -1$ and $s_i = 0$. The energies $\omega_i = \sqrt{\mathbf{p}^2 + m_i^2}$ are calculated with help of the tree-level mass expressions (4) after substituting into them the order parameter values determined in our field theoretical treatment for the two phases, that is, by solving (6)–(8) and (12).

The simple model predicts that Δn_B, Δn_Y, and Δs are always positive, while Δn_I is always negative. Moreover, the following relations are obtained: $\Delta n_B \approx \Delta n_Y$, $\Delta s > \Delta n_B$, and $\Delta s > |\Delta n_I|$. The discontinuity of the particle number densities is determined by the contributions of essentially three quasiparticles: u, d, and $\pi^\pm$. From our simple and transparent model we get the sign and even the magnitude of the shifts of the CEP in agreement with Fig. 4 with the single exception of $d\mu_I/dT$. The ideal gas model does not reproduce the value of this derivative obtained by solving our model. We interpret this discrepancy as a result of the strong coupling between the $\langle \bar{u}u \rangle \sim \sqrt{2/3}v_0 + \sqrt{1/3}v_8 + v_3$ and $\langle \bar{d}d \rangle \sim \sqrt{2/3}v_0 + \sqrt{1/3}v_8 - v_3$ condensates not captured by the ideal gas approximation. As one can check also in [13], the strong coupling between these condensates reduces the temperature of the CEP when a finite μ_I is switched on. This is the same tendency we found in our field theoretical calculation. For the other three shifts it is the mass differences of the lightest quasiparticles of the effective model which exert the strongest influence on the variation of CEP position.

B. Quasiparticle masses

We turn to the study of the dependence of the tree-level masses and the one-loop pole masses on the temperature and the chemical potentials. The one-loop pole masses are determined as the zeros of the real part of the corresponding one-loop inverse propagators at vanishing spatial momentum. For example, the equation determining the one-loop π^+ mass reads $M^2_{\pi^+} = \mathrm{Re}G^{-1}_{\pi^+}(p_0 = M_{\pi^+}, \mathbf{p} = 0)$. If there is more than one solution to this type of equation, then we follow that solution which in the vacuum lies closer to the physical mass. Usually this solution is lost as the temperature increases and some other solution is found.

In Figs. 5(a) and 5(b) we see that the tree-level masses of $\pi^\pm$, π^0 and σ clearly reflect the restoration of the $SU(2)$ symmetry at high temperature. This is not shown by the masses of $a_0^\pm$, a_0^0 and η. We cannot go to higher values of the temperature because at $T \simeq 252$ MeV the nonstrange condensate x decreases below the value of v_3 and the tree-level mass of the u quark turns into negative. At this temperature there is still no sign for the tendency of the $SU(3)$ chiral partners to become degenerate.

In Fig. 5(c) we can see the dependence of the charged and neutral pion masses on the isospin chemical potential. The charged pions have by far the most significant dependence on μ_I from all of the charged pseudoscalar mesons. At $T = \mu_B = 0$ the splitting between π^+ and π^- is controlled by the bubble diagram involving π^+ and π^-, respectively (see Fig. 1), and the splitting point is at $\mu_I \simeq m_\pi$. One can see that at $T = \mu_B = 0$ the mass of π^0 depends mildly on μ_I. This dependence intensifies with the increase of T and μ_B, but it remains true that the dependence on μ_I is less strong than for the case of $m_{\pi^\pm}$. It is interesting to note that for large values of μ_B, when

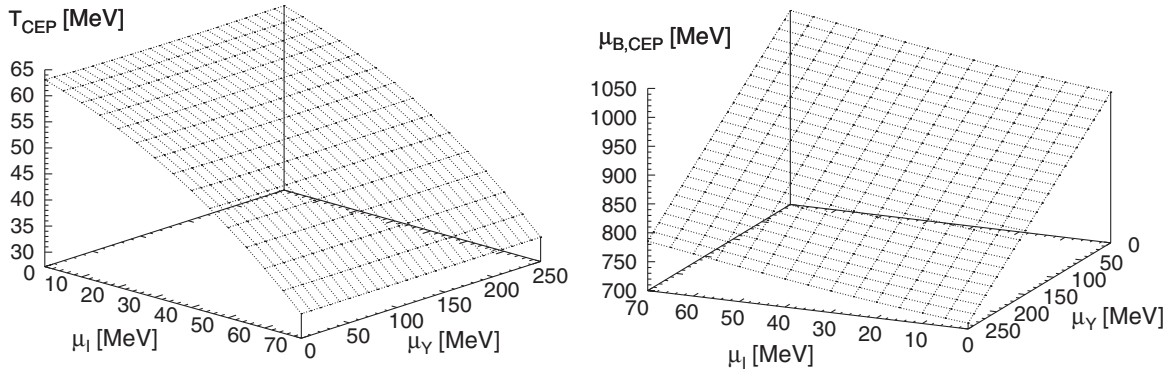

FIG. 4. The surfaces swept by the coordinates T_{CEP} and $\mu_{B,\mathrm{CEP}}$ of the critical end point as a function of μ_I and μ_Y.

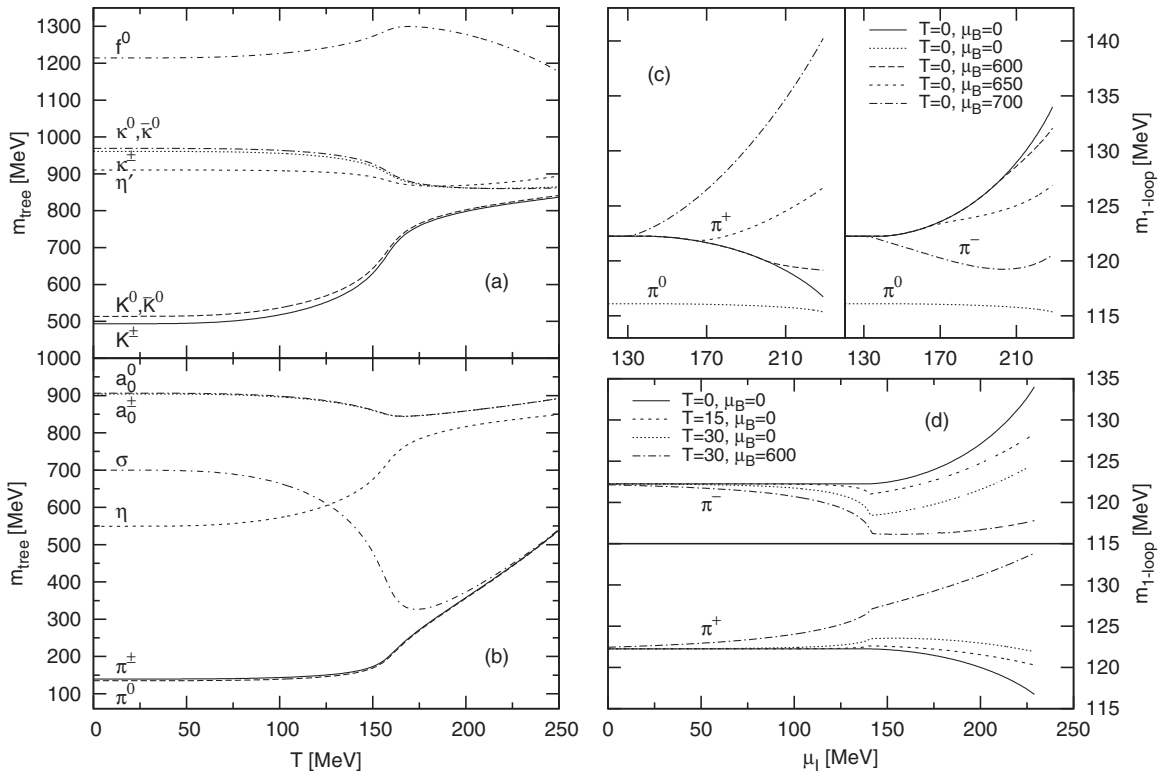

FIG. 5. The temperature dependence of the tree-level masses is shown in panels (a) and (b). The μ_I dependence of the one-loop pion masses for different values of μ_B at $T = 0$ [panel (c)] and $T \neq 0$ [panel (d)].

$\mu_{u/d} > m_{u/d}$ and the fermion bubble contributes to the one-loop self-energies, the shape of the $m_{\pi^\pm}(\mu_I)$ curves changes: m_{π^+} starts to increase with μ_I, and the increase of m_{π^-} with μ_I is slowed down and eventually turned over into a decrease in a given interval of μ_I. Fig.5(d) shows that the increase of the temperature has a similar effect as μ_B in that it turns over the μ_I dependence of $m_{\pi^\pm}$ with respect to the behavior at $T = \mu_B = 0$ starting at a low value of μ_I.

In Fig. 6 we plot, both at the tree and at the one-loop level a combination of the masses and the pion decay constant $\Delta = (m_\eta^2 + m_{\eta'}^2 - 2m_K^2)f_\pi^2/6$, which through the Witten-Veneziano mass formula [34,35]

$$\frac{2N_f}{f_\pi^2}\chi_T = m_\eta^2 + m_{\eta'}^2 - 2m_K^2 \tag{29}$$

with $N_f = 3$, can be considered as an estimation of the topological susceptibility $\chi_T(T)$, which plays a crucial role in the phenomenology of the $U(1)_A$ anomaly (see e.g. [36,37] for recent studies in terms of effective descriptions). In principle $\chi_T(T)$ can also be computed directly in our model if the quantity corresponding to the topological charge density Q_T of the QCD is extracted. This can be done by comparing the four divergence of the singlet axial vector current, which in QCD involves the $U(1)_A$ anomaly term with the corresponding current of the chiral quark model. Since the determinant term of Eq. (1) breaks the $U(1)_A$ symmetry, the correspondence is $Q_T \sim g(\det(M) - \det(M^\dagger)) = g\,\mathrm{Im}\,\det M$.

The decrease with T of the estimated $\chi_T(T)$ seen in Fig. 6 does not mean the restoration of the $U(1)_A$ symme-

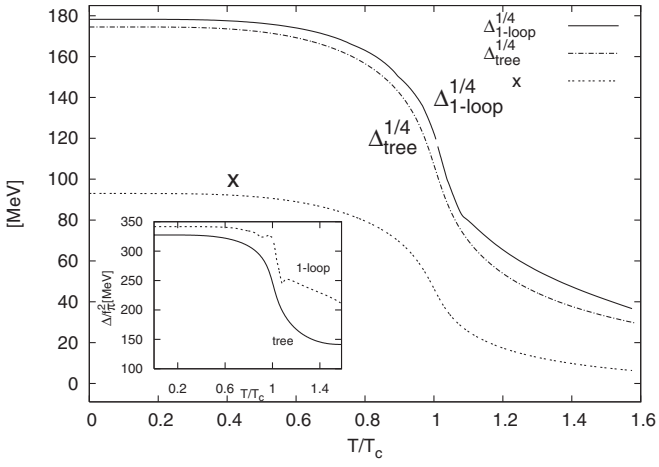

FIG. 6. Estimation of the topological susceptibility through the Witten-Veneziano mass formula using one-loop and tree-level masses. The T-dependent pion decay constant $[f_\pi(T)]$ is approximated with the nonstrange condensate x. The value of the pseudocritical temperature is $T_c = 157.98$ MeV. In the inserted figure, Δ/f_π^2 is plotted based on the tree and one-loop masses.

try, since through $f_\pi(T)$, $\chi_T(T)$ is dominated by the restoration of the chiral symmetry. In view of (29) this can be also seen on the inserted figure of Fig. 6. However, the fact that at $T = 0$ the estimated $\chi_T(T)$ is so close to the value obtained on the lattice in [38] and the curve itself stays within 10% of the lattice points could imply that the effective restoration of the $U(1)_A$ symmetry, if contained in the lattice data,[1] could be implemented in an effective description based on the chiral quark model. In the Nambu-Jona-Lasinio model the lattice result on $\chi_T(T)$ [38] is converted into the temperature dependence of the strength of the determinant term by fitting it with the explicit formula of the susceptibility calculated in [39].

IV. CONCLUSIONS

In this paper we studied the influence of the isospin and hypercharge chemical potentials on the μ_B-T chiral phase diagram of the three flavored chiral constituent quark model with explicitly broken $SU(3)_L \times SU(3)_R$ symmetry. The model was parametrized at the one-loop level, and optimized perturbation theory was used for the resummation of the perturbative series. Only one CEP is found for both spontaneous and explicit isospin breaking. In the latter case, based on the width of the peak of the chiral susceptibility, the crossover transition at $\mu_{B,I,Y} = 0$ is found to be weaker than in the former case. Compared to the case without isospin breaking, in the case with explicit isospin breaking, the location of the CEP moves to a higher value of μ_B and a lower value of T. For $\mu_I = \mu_Y = 0$ the coordinates of the CEP are $(T, \mu_B)_{\mathrm{CEP}} = (63.08, 960.8)$ MeV. This value of $\mu_{B,\mathrm{CEP}}$ is about 3 times larger than the value found on the lattice [40] and increases (decreases) linearly with μ_I (μ_Y), while T_{CEP} is two-fifths of the lattice value and decreases slightly with the increase of μ_Y and significantly with the increase of μ_I. Using an ideal gas picture and the generalized Clausius-Clapeyron equations we could interpret semiquantitatively with one exception the influence of μ_Y and μ_I chemical potentials on the CEP as resulting from the quasiparticle masses. We also studied the dependence of the charged and neutral one-loop pion masses on the isospin chemical potential at different values of the temperature and the baryon chemical potential. As a continuation of the present study, it would be interesting to investigate at what value of the μ_I do the charged pions condensate.

ACKNOWLEDGMENTS

Work was supported by the Hungarian Scientific Research Fund (OTKA) under Contract Nos. T046129 and NI68228. Zs. Sz. is supported by OTKA Postdoctoral Grant No. PD 050015. We thank A. Patkós for discussion and suggestions, especially on the correct way of introducing the various chemical potentials, and for careful reading of the manuscript.

APPENDIX: THE FORMALISM OF RELATIVISTIC MANY-BODY THEORY FOR A SYSTEM AT FINITE DENSITY AND TEMPERATURE

We review below the method of relativistic many-body theory developed in [30] for the perturbative calculation of the self-energy at finite temperature and density.

First we present the derivation of the tree-level Green's functions for K^-, K^+, which depends both on the isospin and hypercharge chemical potentials. The field operators $K^-(x)$ and $K^+(x)$ are written in terms of creation and annihilation operators $a^+(\mathbf{p})$, $b^+(\mathbf{p})$ and $a(\mathbf{p})$, $b(\mathbf{p})$, respectively, as

$$K^-(x) = \int \frac{d^3\mathbf{p}}{(2\pi)^{3/2}} \frac{1}{\sqrt{2E_\mathbf{p}}} (a^+(\mathbf{p}) e^{ip\cdot x} + b(\mathbf{p}) e^{-ip\cdot x}) \Big|_{p_0 = E_\mathbf{p}},$$
$$K^+(x) = \int \frac{d^3\mathbf{p}}{(2\pi)^{3/2}} \frac{1}{\sqrt{2E_\mathbf{p}}} (b^+(\mathbf{p}) e^{ip\cdot x} + a(\mathbf{p}) e^{-ip\cdot x}) \Big|_{p_0 = E_\mathbf{p}}, \tag{A1}$$

where $E_\mathbf{p} = \sqrt{\mathbf{p}^2 + m_{K^\pm}^2}$. This means that $a^+(\mathbf{p})$ creates a K^+ particle, $b^+(\mathbf{p})$ creates a K^- particle, etc. The operators have the usual nonzero commutators

$$[a(\mathbf{p}), a^+(\mathbf{k})] = [b(\mathbf{p}), b^+(\mathbf{k})] = \delta(\mathbf{p} - \mathbf{k}). \tag{A2}$$

The two point functions for K^- and K^+ are defined as

$$\begin{aligned} G_{K^-}(y - x) &:= \langle T K^-(y) K^+(x) \rangle_\beta \\ &= \Theta(y_0 - x_0) \langle K^-(y) K^+(x) \rangle_\beta \\ &\quad + \Theta(x_0 - y_0) \langle K^+(x) K^-(y) \rangle_\beta, \\ G_{K^+}(y - x) &:= \langle T K^+(y) K^-(x) \rangle_\beta \\ &= \Theta(y_0 - x_0) \langle K^+(y) K^-(x) \rangle_\beta \\ &\quad + \Theta(x_0 - y_0) \langle K^-(x) K^+(y) \rangle_\beta, \end{aligned} \tag{A3}$$

where the average is to be taken over a grand canonical ensemble; that is, for an operator O one has

$$\langle O \rangle_\beta = \frac{\mathrm{Tr}[e^{-\beta \mathcal{H}} O]}{\mathrm{Tr} e^{-\beta \mathcal{H}}}, \tag{A4}$$

with $\mathcal{H} = H - \mu_i Q_i$. We make this distinction between K^+ and K^- propagators because the particle and its antiparticle feel differently the presence of the dense medium, resulting in a different mass dependence on the chemical potential. In our case this difference in the mass manifests itself first at one-loop level.

Substituting (A1) into (A3), taking only the noninteracting part of the Hamiltonian H, with the help of the commutator relations given in (A2) and the Campbell-Baker-

[1] Restoration of $U(1)_A$ symmetry requires that $\chi_T(T)$ decreases faster than $f_\pi(T)$ with the increase of T so that $\chi_T(T)/f_\pi^2(T) \to 0$.

Hausdorff relation one evaluates the expectation values obtaining

$$\begin{aligned}\langle a^+(\mathbf{p})a(\mathbf{q})\rangle_\beta &= \delta(\mathbf{p}-\mathbf{q})n_{K^+}(E_\mathbf{p}),\\ \langle b^+(\mathbf{p})b(\mathbf{q})\rangle_\beta &= \delta(\mathbf{p}-\mathbf{q})\bar{n}_{K^+}(E_\mathbf{p}),\end{aligned} \tag{A5}$$

where $n_{K^+}(E_\mathbf{p}) = \frac{1}{e^{\beta(E_\mathbf{p}-\mu_{K^+})}-1}$, $\bar{n}_{K^+}(E_\mathbf{p}) = \frac{1}{e^{\beta(E_\mathbf{p}+\mu_{K^+})}-1}$. Note, that $\bar{n}_{K^+}(E_\mathbf{p}) = n_{K^-}(E_\mathbf{p})$. Using (A5) and the Fourier representation of $\Theta(t)$ in (A3) one obtains in momentum space the K^+ and K^- propagators given in (25).

Next, we calculate a one-loop bosonic bubble appearing in Fig. 1. With the standard rules of the perturbation theory, using the conventions of [41] the π^+ self-energy is given by

$$\begin{aligned}-i\Sigma_{\pi^+}(y,x) = &-4(3\tilde{G}_{2\beta\gamma} + 4\tilde{H}_{2\beta,\gamma\delta}\upsilon_\delta)\\ &\times(3\tilde{G}_{1\beta'\gamma'} + 4\tilde{H}_{1\beta',\gamma'\delta'}\upsilon_{\delta'})\\ &\times G_{\pi_{\beta'}\pi_\beta}(y,x)G_{\sigma_{\gamma'}\sigma_\gamma}(y,x).\end{aligned} \tag{A6}$$

The first nonmixing bubble graph in the diagrammatic representation of Σ_{π^+} given in Fig. 1 is obtained with the choice $\beta = 4$, $\beta' = 5$ implying $\gamma = 7$, $\gamma' = 6$. Using that $\tilde{G}_{156} = \tilde{G}_{247}$ and $\tilde{H}_{15,6\delta} = \tilde{H}_{24,7\delta}$ the contribution of this graph is

$$-i\Sigma^{K^+\bar{\kappa}^0}_{\pi^+}(y,x) = \pi^- \to \pi^+ \langle x \rangle \kappa^0 \to K^- \quad \bar{\kappa}^0 \to \langle y \rangle \pi^- \to \pi^+ = -4\left[3\tilde{G}_{247} + 4\tilde{H}_{24,7\delta}\upsilon_\delta\right]^2 G_{K^+K^-}(y,x)G_{\bar{\kappa}^0\kappa^0}(y,x). \tag{A7}$$

The labels in the graph denote the field operators, e.g. on the left-hand side π^- creates a π^+ particle.

Going to momentum space one has

$$\begin{aligned}\Sigma^{K^+\bar{\kappa}^0}_{\pi^+}(p) &= -4iV^2_{\pi^+K^-\kappa^0}\int\frac{d^4k}{(2\pi)^4}G_{K^+}(k)G_{\bar{\kappa}^0}(p-k)\\ &= 4V^2_{\pi^+K^-\kappa^0}I^\beta_B(p, m_{K^+}, \mu_{K^+}, m_{\bar{\kappa}^0}, \mu_{\bar{\kappa}^0}),\end{aligned} \tag{A8}$$

where the vertex is $V_{\pi^+K^-\kappa^0} = 4[\frac{c}{\sqrt{2}} + \frac{f_2}{\sqrt{3}}\upsilon_0 - \sqrt{2}f_2(\frac{\upsilon_8}{\sqrt{3}} - \upsilon_3)]$, and $G_{K^+}(k) \equiv G_{K^+K^-}(k)$.

Generally, at finite chemical potentials and temperature for a bosonic bubble diagram one calculates at vanishing spatial external momentum ($\mathbf{p} = 0$) an integral of the form

$$\begin{aligned}&I^\beta_B(p_0, m_1, \mu_1, m_2, \mu_2)\\ &= -i\int\frac{d^4k}{(2\pi)^4}G_1(k)G_2(p-k)\Big|_{\mathbf{p}=0}\\ &= \int\frac{d^3\mathbf{k}}{(2\pi)^3}\frac{1}{4E_1E_2}\left[\frac{1+n_1+n_2}{p_0-E_1-E_2} - \frac{n_1-\bar{n}_2}{p_0-E_1+E_2}\right.\\ &\quad\left. + \frac{\bar{n}_1-n_2}{p_0+E_1-E_2} - \frac{1+\bar{n}_1+\bar{n}_2}{p_0+E_1+E_2}\right],\end{aligned} \tag{A9}$$

where for the propagators one uses a form similar to that in (25) and to arrive at the second equality one performs a contour integration in the complex energy plane. The distribution functions $n_i \equiv n_i(E_i)$ with $E_i = \sqrt{\mathbf{k}^2 + m_i^2}$ contain the chemical potential for particle or antiparticle which is created by the fields of the vertex in the left-hand side.

We rewrite the integral (A9) as

$$\begin{aligned}&I^\beta_B(p_0, m_1, \mu_1, m_2, \mu_2)\\ &= I^{\mu,T=0}_B(p_0, m_1, m_2) + \frac{1}{8\pi^2 p_0}\sum_{i=1}^{2}\mathcal{P}\int_{m_i}^{\infty}dE\sqrt{E^2-m_i^2}\\ &\quad\times\left[\frac{n_i(E)}{p_0a_i - E} + \frac{\bar{n}_i(E)}{p_0a_i + E}\right],\end{aligned} \tag{A10}$$

where the remaining integral is evaluated numerically and $\mathcal{P}$ stands for principal value. The vacuum integral $I^{\mu,T=0}_B(p_0, m_1, m_2)$ is given by the expression (B4) of [19], $n_i = 1/(\exp(\beta(E-\mu_i)) - 1)$ is the Bose-Einstein distribution and $a_i = [1 + (-1)^{i-1}(m_1^2 - m_2^2)/p_0^2]/2$.

For fermions the method is identical to that used for the bosons. The fermion propagators for the constituent quarks u, $\bar{u}$ are defined as

$$\begin{aligned}D_u(y-x) &:= \langle Tu(y)\bar{u}(x)\rangle_\beta\\ &= \Theta(y_0-x_0)\langle u(y)\bar{u}(x)\rangle_\beta\\ &\quad - \Theta(x_0-y_0)\langle\bar{u}(x)u(y)\rangle_\beta,\\ D_{\bar{u}}(y-x) &:= \langle T\bar{u}(y)u(x)\rangle_\beta = \Theta(y_0-x_0)\langle\bar{u}(y)u(x)\rangle_\beta\\ &\quad - \Theta(x_0-y_0)\langle u(x)\bar{u}(y)\rangle_\beta,\end{aligned} \tag{A11}$$

which in the momentum space read

$$D_u(k) = \frac{i(\not{k} + m_u)}{2E_{\mathbf{k}}}\left[\frac{1 - f_u^+(E_{\mathbf{k}})}{k_0 - E_{\mathbf{k}} + i\epsilon} + \frac{f_u^+(E_{\mathbf{k}})}{k_0 - E_{\mathbf{k}} - i\epsilon} - \frac{1 - f_u^-(E_{\mathbf{k}})}{k_0 + E_{\mathbf{k}} - i\epsilon} - \frac{f_u^-(E_{\mathbf{k}})}{k_0 + E_{\mathbf{k}} + i\epsilon}\right],$$
$$D_{\bar{u}}(k) = \frac{i(\not{k} + m_u)}{2E_{\mathbf{k}}}\left[\frac{1 - f_u^-(E_{\mathbf{k}})}{k_0 - E_{\mathbf{k}} + i\epsilon} + \frac{f_u^-(E_{\mathbf{k}})}{k_0 - E_{\mathbf{k}} - i\epsilon} - \frac{1 - f_u^+(E_{\mathbf{k}})}{k_0 + E_{\mathbf{k}} - i\epsilon} - \frac{f_u^+(E_{\mathbf{k}})}{k_0 + E_{\mathbf{k}} + i\epsilon}\right], \tag{A12}$$

where $f_u^+(E_{\mathbf{p}}) = \frac{1}{e^{\beta(E_{\mathbf{p}} - \mu_u)} + 1}$ and $f_u^-(E_{\mathbf{p}}) = \frac{1}{e^{\beta(E_{\mathbf{p}} + \mu_u)} + 1}$ are the distribution functions for u type quarks and antiquarks.

Then for the fermionic bubble appearing in the π^+ self-energy (see Fig. 1) one has

$$\Sigma_{\pi^+}^{u\bar{d}}(p) = -\frac{g_F^2}{2} N_c i\mathrm{Tr}\int \frac{d^4k}{(2\pi)^4}\gamma_5 D_{\bar{d}}(k) D_u(k + p) = \frac{g_F^2}{2} N_c I_F^{\beta}(p, m_d, \mu_{\bar{d}}, m_u, \mu_u). \tag{A13}$$

Similarly to Eq. (A9) in case of fermions we use the integral:

$$\begin{aligned}
&I_F^{\beta}(p_0, m_1, \mu_1, \mu_2, m_2) \\
&= -i\mathrm{Tr}\int_k \gamma_5 D_1(k)\gamma_5 D_2(k + p)\Big|_{\mathbf{p}=0} \\
&= \int \frac{d^3\mathbf{k}}{(2\pi)^3}\left[\frac{1}{E_1}(f_1^+ + f_1^- - 1) + \frac{1}{E_2}(f_2^+ + f_2^- - 1)\right] + 2(p_0^2 - (m_1 - m_2)^2) \\
&\quad \times \int \frac{d^3\mathbf{k}}{(2\pi)^3}\frac{1}{4E_1E_2}\left[\frac{1 - f_1^+ - f_2^+}{p_0 - E_1 - E_2} + \frac{f_1^+ - f_2^-}{p_0 - E_1 + E_2} - \frac{f_1^- - f_2^+}{p_0 + E_1 - E_2} - \frac{1 - f_1^- - f_2^-}{p_0 + E_1 + E_2}\right] \\
&= -2T_F^{\mu,T=0}(m_1) - 2T_F^{\mu,T=0}(m_2) + 2(p_0^2 - (m_1 - m_2)^2) I_B^{\mu,T=0}(p_0, m_1, m_2) + T_F^{T\neq 0}(m_1) + T_F^{T\neq 0}(m_2) \\
&\quad - \frac{p_0^2 - (m_1 - m_2)^2}{4\pi^2 p_0}\sum_{i=1}^{2}\mathcal{P}\int_{m_i}^{\infty} dE\sqrt{E^2 - m_i^2}\left[\frac{f_i^+(E)}{p_0 a_i - E} + \frac{f_i^-(E)}{p_0 a_i + E}\right],
\end{aligned} \tag{A14}$$

where $f_i^{\pm} = 1/(\exp(\beta(E \mp \mu_i)) + 1)$ is the Fermi-Dirac distribution.

[1] P. Braun-Munzinger, J. Stachel, J. P. Wessels, and N. Xu, Phys. Lett. B **344**, 43 (1995).
[2] P. Braun-Munzinger, I. Heppe, and J. Stachel, Phys. Lett. B **465**, 15 (1999).
[3] F. Becattini, M. Gaździcki, and J. Sollfrank, Eur. Phys. J. C **5**, 143 (1998).
[4] P. Senger *et al.*, Proc. Sci., CPOD2006 (2006) 018.
[5] J. Rafelski and B. Muller, Phys. Rev. Lett. **48**, 1066 (1982).
[6] C. Greiner and S. Leupold, J. Phys. G **27**, L95 (2001).
[7] D. Toublan, B. Klein, and J. J. M. Verbaarschot, Nucl. Phys. B, Proc. Suppl. **140**, 562 (2005).
[8] M. Alford, A. Kapustin, and F. Wilczek, Phys. Rev. D **59**, 054502 (1999).
[9] B. Klein, D. Toublan, and J. J. M. Verbaarschot, Phys. Rev. D **68**, 014009 (2003).
[10] D. Toublan and J. B. Kogut, Phys. Lett. B **564**, 212 (2003).
[11] Y. Nishida, Phys. Rev. D **69**, 094501 (2004).
[12] A. Barducci, G. Pettini, L. Ravagli, and R. Casalbuoni, Phys. Lett. B **564**, 217 (2003).
[13] M. Frank, M. Buballa, and M. Oertel, Phys. Lett. B **562**, 221 (2003).
[14] L. He and P. Zhuang, Phys. Lett. B **615**, 93 (2005).
[15] D. Toublan and J. B. Kogut, Phys. Lett. B **605**, 129 (2005).
[16] A. Jakovác, A. Patkós, Zs. Szép, and P. Szépfalusy, Phys. Lett. B **582**, 179 (2004).
[17] T. Herpay, A. Patkós, Zs. Szép, and P. Szépfalusy, Phys. Rev. D **71**, 125017 (2005).
[18] T. Herpay and Zs. Szép, Phys. Rev. D **74**, 025008 (2006).
[19] P. Kovács and Zs. Szép, Phys. Rev. D **75**, 025015 (2007).
[20] D. T. Son and M. A. Stephanov, Phys. Rev. Lett. **86**, 592 (2001).
[21] J. B. Kogut, D. Toublan, and D. K. Sinclair, Phys. Rev. D **68**, 054507 (2003).
[22] D. K. Sinclair, J. B. Kogut, and D. Toublan, Prog. Theor. Phys. Suppl. **153**, 40 (2004).
[23] L. He, M. Jin, and P. Zhuang, Phys. Rev. D **71**, 116001 (2005).
[24] H. J. Warringa, D. Boer, and J. O. Andersen, Phys. Rev. D **72**, 014015 (2005).
[25] D. K. Sinclair and J. B. Kogut, Proc. Sci. LAT2006 (2006) 147.
[26] J. O. Andersen, Phys. Rev. D **75**, 065011 (2007).
[27] L.-H. Chan and R. W. Haymaker, Phys. Rev. D **7**, 402 (1973).

[28] J. T. Lenaghan, D. H. Rischke, and J. Schaffner-Bielich, Phys. Rev. D **62**, 085008 (2000).
[29] S. Chiku and T. Hatsuda, Phys. Rev. D **58**, 076001 (1998).
[30] R. L. Bowerst and R. L. Zimmerman, Phys. Rev. D **7**, 296 (1973).
[31] Y. Aoki, Z. Fodor, S. D. Katz, and K. K. Szabó, Phys. Lett. B **643**, 46 (2006).
[32] M. A. Halasz *et al.*, Phys. Rev. D **58**, 096007 (1998).
[33] S. Gupta, arXiv:0712.0434.
[34] E. Witten, Nucl. Phys. **B156**, 269 (1979).
[35] G. Veneziano, Nucl. Phys. **B159**, 213 (1979).
[36] P. Costa, M. C. Ruivo, C. A. de Sousa, and Yu. L. Kalinovsky, Phys. Rev. D **71**, 116002 (2005).
[37] D. Horvatic, D. Klabucar, and A. E. Radzhabov, Phys. Rev. D **76**, 096009 (2007).
[38] B. Allés, M. D'Elia, and A. Di Giacomo, Nucl. Phys. **B494**, 281 (1997); **B679**, 397 (2004).
[39] K. Ohnishi, K. Fukushima, and K. Ohta, Phys. Rev. C **63**, 045203 (2001).
[40] Z. Fodor and S. D. Katz, J. High Energy Phys. 04 (2004) 050.
[41] M. E. Peskin and D. V. Schoeder, *An Introduction to Quantum Field Theory* (Addison Wesley, Reading, MA, 1995).